Boson description of low-lying collective states in ^{128}Ba

H. Sakamoto
Faculty of Engineering, Gifu University, Gifu 501-1193, Japan
(Received 16 October 2015; revised manuscript received 14 January 2016; published 11 March 2016)

The low-lying collective states in ^{128}Ba are investigated microscopically by means of the boson expansion theory with the self-consistent effective interactions. Calculated level structures and electromagnetic properties are compared with the experimental data. Theoretical structures of the collective wave functions are illustrated in detail for 0_1^+, 0_2^+, 0_3^+, 2_1^+, 2_2^+, and 2_3^+ states. In the present results, the main contribution to the 0_2^+ state of ^{128}Ba comes from the three-phonon component, and the two-phonon component is rather dominant in the 0_3^+ state. The description of the wave functions is compared to the results of the general collective model.

DOI: 10.1103/PhysRevC.93.034315

I. INTRODUCTION

The neutron-deficient Ba nuclei are known as typical examples of transitional nuclei and provide a good testing ground for various theoretical models of nuclear collective motions [1–5]. There have been suggestions that some of the lighter Ba nuclei could have nearly-γ-unstable structures [6–9]. In this mass region, attention has been focused on the interplay of γ softness and triaxiality [3,10–12], and there have been interesting discussions on the nature of the low-lying 0^+ states [4,13–15]. It was noticed [4,13] that the low-lying 0^+ states in the $A = 130$ mass region could have a more complicated nature than the one implied by the simple geometrical interpretation in terms of β or (two-phonon) γ vibrations. Asai *et al.* [14] identified, in the EC/β^+ experiment with a high-efficiency detector system, the 0_2^+ states and a number of higher-excited 0^+ states in ^{124,126,128,130}Ba and clarified that the level energy of the 0_2^+ state in neutron-deficient Ba nuclei has a minimum at $N = 72$. It was suggested [14] that the energy staggering index [13] of the quasi-γ band indicates the highest degree of γ instability at ^{128}Ba in this region, which may be associated with the lower 0_2^+ level energy around ^{128}Ba.

As pointed out by Petkov *et al.* [16], it has been an open and challenging problem for the microscopic collective models to describe in a consistent way all observed properties of the low-lying collective states. We have been interested in this problem and, for the structures of the low-lying collective states in Ba isotopes, we reported in Refs. [17–19] results of our studies based on the boson expansion theory (BET) along the lines of Kishimoto–Tamura [1,20,21]. In the previous reports, calculated potential surfaces, level energies, electromagnetic and several related properties have been presented and discussed, but there has been few illustrations of the structures of the collective wave functions. Thus it is advisable to take an overall look at the above problem from the present point of view having detailed descriptions of the wave functions of low-lying collective states. The present paper is devoted to this purpose and aims at illustrating the structures of boson wave functions, which hopefully help to understand microscopically the features of the low-lying collective states in ^{128}Ba.

II. THEORETICAL FRAMEWORK

The theoretical framework is discussed in detail in Refs. [19,22]; here it is described only briefly. The calculation in this paper is performed based on the normal-ordered linked-cluster BET of Kishimoto–Tamura [1,20,21] with several refinements developed in Refs. [23,24]. The BET allows one to take into account higher-order terms neglected in the random-phase approximation (RPA), and the adiabatic condition for particle motions can be avoided. It is a very promising method for the microscopic description of anharmonicities in nuclear quadrupole collective motions, if the coupling to noncollective states are faithfully included in the calculation.

The model Hamiltonian with which the present analyses start is given in fermion operators as Eq. (1) of Ref. [19]. The single-particle base is constructed by using the spherical limit of the Nilsson Hamiltonian [25], and the model space is spanned by $2p_{1/2}$, $2p_{3/2}$, $1f_{5/2}$, $3s_{1/2}$, $2d_{3/2}$, $2d_{5/2}$, $1g_{7/2}$, $1g_{9/2}$, and $1h_{11/2}$ orbits for protons and by $3s_{1/2}$, $2d_{3/2}$, $2d_{5/2}$, $1g_{7/2}$, $2f_{7/2}$, $1h_{9/2}$, $1h_{11/2}$, and $1i_{13/2}$ orbits for neutrons.

The residual interactions comprised in the fermion Hamiltonian are the monopole- and quadrupole-pairing interactions, the quadrupole-quadrupole (QQ) interaction, and the effective three- and four-body interactions. The effective many-body interactions have been introduced as the higher-order terms of the QQ interaction to recover the saturation and the self-consistency between the density and the potential in higher-order accuracy (*nuclear self-consistency*) [26–31]. The same type of many-body interactions have been independently derived by Marshalek [32], and the three-body interaction has been applied to study anharmonicities in nuclear quadrupole collective motions by several authors [33–36].

Strengths of the monopole-pairing interactions, $G_0(p)$ for protons and $G_0(n)$ for neutrons, are determined to fit the experimental gap energies through the BCS gap equation. The adopted strengths in the present calculations are $G_0(p) = 24.37/A$ MeV for protons and $G_0(n) = 21.74/A$ MeV for neutrons, and corresponding gap energies are $\Delta_p = 1.333$ MeV and $\Delta_n = 1.366$ MeV, respectively. These strengths are nearly compatible with the systematics proposed by Copnell *et al.* [37] and are in between the two different parameter sets, the standard pairing strengths (SPS) and the weak pairing

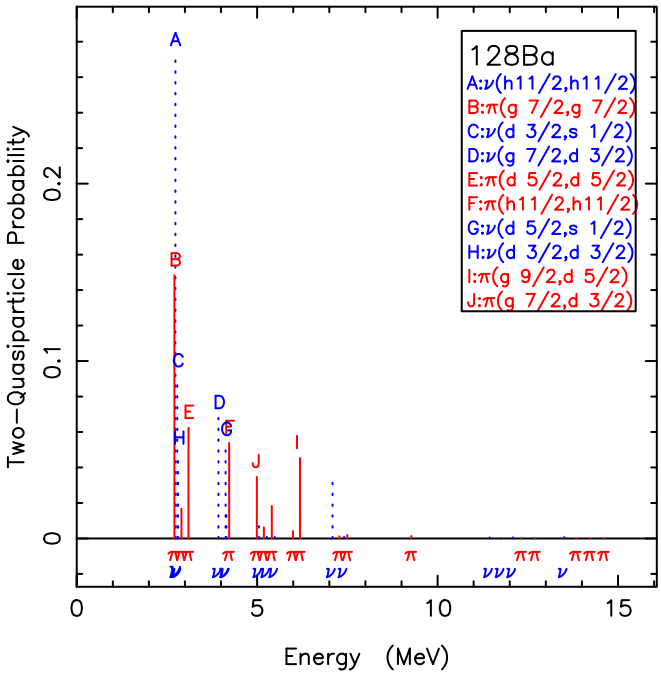

FIG. 1. The two-quasiparticle probabilities in the adiabatic collective Tamm–Dancoff mode for the case of ^{128}Ba are plotted against the two-quasiparticle energies. The scripts π and ν are attached to distinguish the proton components (solid red lines) and the neutron components (dotted blue lines).

strengths (WPS) investigated in the microscopic calculations by Rohoziński *et al.* [2].

The strengths of the quadrupole-pairing interactions are parametrized as $g_2'(p) = G_2(p)/G_2^{\rm self}(p)$, $g_2'(n) = G_2(n)/G_2^{\rm self}(n)$, where $G_2^{\rm self}(p)$ for protons and $G_2^{\rm self}(n)$ for neutrons are the self-consistent strengths of the quadrupole-pairing interaction to recover the *local Galilean invariance* in the RPA order [38]. The strengths of the QQ interaction and its higher-order terms $\chi^{(2)}$, $\chi^{(3)}$, and $\chi^{(4)}$ are parametrized as $f_2 = \chi^{(2)}/\chi_2^{\rm self}$, $f_3 = \chi^{(3)}/\chi_3^{\rm self}$, $f_4 = \chi^{(4)}/\chi_4^{\rm self}$, where $\chi_2^{\rm self}$, $\chi_3^{\rm self}$, and $\chi_4^{\rm self}$ are the self-consistent values of $\chi^{(2)}$, $\chi^{(3)}$, and $\chi^{(4)}$, respectively, which are derived in Ref. [31]. In the present analyses, to reduce the number of free parameters, these parameters are set to $f_2 = f_3 = f_4$ and $g_2'(p) = g_2'(n) = g_2'$, and in calculating the energy spectra the two dimensionless parameters, f_2 and g_2', are varied slightly around the vicinity of the predicted value, i.e., unity.

It was emphasized in Refs. [21,39] that a meaningful BET should start from a fermion system described in terms of Tamm–Dancoff (TD) representation or its equivalent. In this work, as a choice of the collective coordinates, the so-called adiabatic TD mode [24] is adopted. In Fig. 1 the two-quasiparticle probabilities in the adiabatic collective TD mode for the case of ^{128}Ba are plotted against the two-quasiparticle energies of protons (π) and neutrons (ν). Possibilities of different choices of the representation were investigated in Ref. [24], and it was shown that the noncollective couplings play crucial roles to stabilize the results of numerical calculations and to remove the sensitive dependence on the particular choice of the collective coordinates.

By use of the BET, the original fermion Hamiltonian is mapped to the corresponding boson Hamiltonian and is expanded up to fourth-order with respect to the collective boson. Since the quasiparticle representation is used in the present formalism of BET, it suffers from the spurious particle-number excitations associated with particle-number nonconservation. To remove such spurious modes, the prescription developed in Ref. [23] is used. In the collective Hamiltonian, coupling effects between the collective and the noncollective modes are approximately included by using the perturbation theory for a quasidegenerate system [30,40–43] with the Feshbach formalism [44]. Then the resultant collective Hamiltonian is diagonalized in the collective subspace of the boson Hilbert space to obtain energy spectra as well as boson wave functions for low-lying collective states. The basis vectors of the collective subspace are expressed as $|N v \eta I M)$, where N is the boson number, v is the seniority number, I is the spin with its projection M, and η is an additional quantum number necessary for a complete labeling of the basis vectors. In the present numerical calculations, states with $N \leqslant 18$ have been taken, which amount to a diagonalization space of slightly less than 100-dimensional matrices for each spin I. In drawing potential-energy surfaces to visualize the physical properties described by the collective Hamiltonian, the collective quadrupole boson operators $\alpha_{2\mu}^\dagger$ and $\alpha_{2\mu}$ are transformed into the momentum and conjugate coordinate operators, $\pi_{2\mu}$ and $\beta_{2\mu}$, as defined in Refs. [1,22] and an equivalent expression of the collective Hamiltonian is derived in terms of π and β. In the boson expansion approach, the adiabatic assumption is not made and generally terms appear that are higher power in π. Such terms give corrections to the theories based on the adiabatic assumption.

III. RESULTS AND DISCUSSION

As stated earlier, there are two adjustable parameters f_2 and g_2' to fit energy spectra and, in studying electromagnetic properties, a quadrupole effective charge $e_{\rm eff}$ is introduced as the only additional parameter in this paper to fit the experimental data. It should be noted that some slightly different sets of f_2, g_2' values may often be possible to obtain nearly compatible fits [1]. The effects of varying these interaction strengths on the low-lying collective states were reported in Ref. [22] for the case of neutron-deficient doubly even xenon isotopes. However, since the present purpose is not to find the best parameter set just to fit a single nucleus, in the following we will not play too much with these parameters but would rather select one of the interesting and acceptable cases of $f_2 = 1.03$, $g_2' = 0.895$, and $e_{\rm eff} = 0.5e$ for ^{128}Ba and investigate level energies, structures of boson wave functions, and electromagnetic properties of low-lying collective states. In fact, as will be shown promptly, the case corresponds to a typical situation of a γ-soft potential having two axial minima with nearly equal depths. For comparison, it is estimated for the QQ interaction that the RPA critical strength is $f_2^{\rm RPA}({\rm crit}) = 0.848$, while the strength to fit the experimental 2_1^+ energy within the RPA is $f_2^{\rm RPA}(2_1^+) = 0.842$.

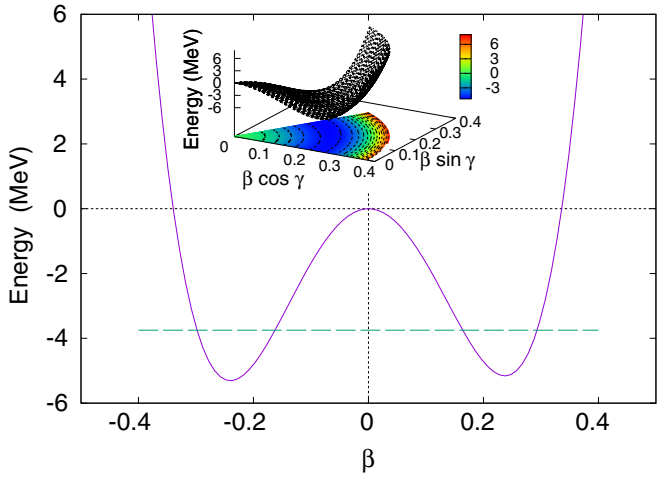

FIG. 2. Calculated potential-energy surface for ^{128}Ba. The horizontal dashed line at -3.75 MeV in the main figure indicates the calculated ground-state energy. The inserted figure shows the contour plot of the potential, where incremental contours (dashed lines) start at -5 MeV stepping by 1 MeV, and there is a valley connecting the prolate minimum ($\beta^{\rm P}_{\rm min} = 0.238$, $V^{\rm P}_{\rm min} = -5.16$ MeV) and the oblate minimum ($\beta^{\rm O}_{\rm min} = -0.240$, $V^{\rm O}_{\rm min} = -5.31$ MeV).

Figure 2 illustrates the calculated potential-energy surface as a function of quadrupole deformation β for ^{128}Ba. This potential surface has two axial minima, one on the prolate side ($\beta^{\rm P}_{\rm min} = 0.238$, $V^{\rm P}_{\rm min} = -5.16$ MeV) and the other on the oblate side ($\beta^{\rm O}_{\rm min} = -0.240$, $V^{\rm O}_{\rm min} = -5.31$ MeV). As shown in the contour plot inserted in Fig. 2, the potential varies monotonically with γ. The difference in depth on both sides, $V^{\rm PO} = V^{\rm O}_{\rm min} - V^{\rm P}_{\rm min}$, is -0.15 MeV; the absolute value of it is rather small compared to the energy of the zero-point oscillation, 1.56 MeV, evaluated relative to the absolute minimum of the potential. This feature of the potential surface implies strong softness or instability for the γ deformation.

Theoretical energy levels are presented in Fig. 3 and compared with experimental data. The energies of the ground-state band and staggering of the quasi-γ band are qualitatively

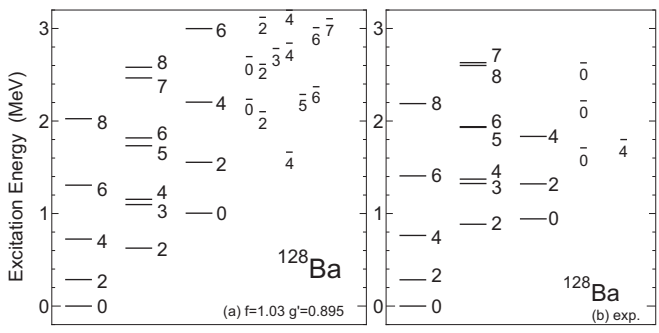

FIG. 3. (a) Calculated energy levels for ^{128}Ba. All the resulting states with $E_x \leqslant 3.2$ MeV and $I \leqslant 8$ are listed: the states in the ground-state band, the quasi-γ band, or the 0^+_2 band are separately accumulated, while other states (short bars) are assembled in their spin groups in columnar forms. For comparison, experimental levels are plotted in panel (b).

reproduced, although the energy of the band head 2^+ state of the γ band is too low. It was reported in Ref. [17] for the case of ^{124}Ba that a small raise (about 1 MeV) of the single-particle energy of $\pi h_{11/2}$ orbit can remedy similar discrepancy; however, in this work all the single-particle energies are simply fixed. In neutron-deficient even-even barium isotopes, bunching of experimental levels ($3^+_\gamma - 4^+_\gamma, 5^+_\gamma - 6^+_\gamma, 7^+_\gamma - 8^+_\gamma$) is prominent. In ^{128}Ba the spacings of these pair states become narrowest and the orders of even- and odd-spin states invert above the 7^+_γ state. This unique feature of inversion is possibly due to the coupling to the two-quasiparticle states which lie closely to the collective states, and this feature is beyond the scrutiny of this work.

It would be interesting and instructive to compare the calculations of the present work with those of the general collective model (GCM). In Ref. [4], Petkov *et al.* applied the GCM to the Ba isotopes and obtained a good description of level schemes and the staggering effect in the quasi-γ bands. The kinetic part of the GCM Hamiltonian is comprised only of second-order terms of π, while the potential part of it is considered up to the sixth-order terms of β, and there are eight adjustable coefficients in their total Hamiltonian. On the other hand, in this work, since the mapped Hamiltonian is expanded up to the fourth-order terms of the collective boson operators, the kinetic part of the boson Hamiltonian contains up to the fourth-order terms of π, although the potential part of it contains at most fourth-order terms of β, and all the coefficients in the total Hamiltonian are determined as functions of f_2 and g'_2, which are the only two adjustable parameters in the present model Hamiltonian.

The potential surface of the GCM for ^{128}Ba [4] seems to possess the softness for the γ deformation, having an absolute minimum at $\beta^{\rm P}_{\rm min} = 0.270$, $V^{\rm P}_{\rm min} = -4.8$ MeV with a prolate-oblate energy difference of 1.6 MeV. While, as already mentioned, the present potential also has the γ softness but with a rather smaller prolate-oblate energy difference. It should be noted here that a strong correlation between the potential-energy surface and the energy spectrum holds only under the condition that all the anharmonic terms in a generalized kinetic part of a collective Hamiltonian, i.e., those terms except the π^2 term, are sufficiently small. If such a condition is not met, to predict the energy spectrum only from the shape of the potential surface can be dangerous [1,24].

In Table I, the theoretical $B(E2)$ values and static quadrupole moments of the low-lying states in ^{128}Ba are listed and are compared with experimental data and the predictions of the GCM [4]. Here one sees impressive similarities between the results of the GCM and those of the present work for the intraband transitions, although there are some sensible differences between the results of the two theories for the static moments and interband transitions. For the ground-state band (g.s.b.), the experimental intraband transitions show relatively high $B(E2 : 4^+_1 \rightarrow 2^+_1)$ value and the following drop, and both theories fail to explain this feature. This experimental feature, which indicates that the quadrupole collectivity of the g.s.b. of ^{128}Ba is suppressed and hits a ceiling at such a low-spin region, is outstandingly unique. It reminds one of the finite-size effect of the interacting boson model (IBM), and Petkov *et al.* [16] suggested that the

TABLE I. Electromagnetic properties of ^{128}Ba. The values given are $B(E2)$ in $(e\,b)^2$, except for those that have the same initial and final states, and in that case they are static quadrupole moments in $e\,b$. An asterisk is attached to a $B(E2)$ value of the present work (BET) if the sign of the corresponding matrix element is negative. For comparison, the results of the general collective model (GCM) [4] are listed. Also, the results of the IBM studied by Wolf *et al.* [15] are listed, where a sharp is attached to a $B(E2)$ value if the corresponding transition is forbidden in the pure O(6) limit.

Transition	I_i	I_f	BET	GCM	Wolf	Expt.[a]
g → g	2	0	0.285	0.276	0.27	$0.275^{+0.026}_{-0.022}$
	2	2	−0.111	−0.876		
	4	2	0.417	0.420		$0.414^{+0.019}_{-0.018}$
	4	4	−0.186	−1.047		
	6	4	0.502	0.495		$0.383^{+0.040}_{-0.033}$
	6	6	−0.243	−1.042		
	8	6	0.565	0.541		$0.367^{+0.056}_{-0.043}$
	8	8	−0.296	−0.917		
$\gamma \to \gamma$	2	2	0.077	0.770		
	3	2	0.344	0.364	0.30	
	3	3	0.5×10^{-7}			
	4	2	0.257*	0.207	0.21	$0.192^{+0.017}_{-0.014}$
	4	3	0.003*			
	4	4	−0.009	0.294		
	5	3	0.286	0.284		
	5	4	0.128*			
	5	5	−0.111	0.400		
	6	4	0.375*	0.317		$0.390^{+0.053}_{-0.041}$
	6	5	0.003			
	6	6	−0.083	0.195		
	7	5	0.402	0.409		
	7	6	0.068			
	7	7	−0.173	0.507		
	8	6	0.451*	0.378		$0.503^{+0.295}_{-0.136}$
	8	7	0.003*			
	8	8	−0.106	0.191		
$0_2^+ \to 0_2^+$	2	0	0.195*	0.175	0.14	
	2	2	−0.051	0.189		
	4	2	0.288	0.242	0.18	
	4	4	−0.089			
	6	4	0.360*			
	6	6	−0.089			
$\gamma \to g$	2	0	0.3×10^{-4}*		0.040#	$0.012^{+0.002}_{-0.001}$
	2	2	0.404*	0.152	0.37	$0.131^{+0.015}_{-0.012}$
	2	4	0.0008			
	3	2	0.0002		0.040#	
	3	4	0.132*		0.12	
	4	2	0.4×10^{-4}*		0.029#	$0.32^{+0.03}_{-0.02} \times 10^{-2}$
	4	4	0.226		0.19	0.061(6)[b]
	5	4	0.0002			
	5	6	0.118*			
	6	4	0.4×10^{-4}*			$0.33^{+0.05}_{-0.04} \times 10^{-2}$
	6	6	0.165*			
	7	8	0.099*			
	8	6	0.0001			$0.41^{+0.24}_{-0.11} \times 10^{-2}$
	8	8	0.128			
$0_2^+ \to g$	0	2	0.0054*			
	2	0	0.0002		0.0#	
	2	2	0.1×10^{-5}*		0.0#	
	2	4	0.003		0.011#	

TABLE I. (*Continued.*)

Transition	I_i	I_f	BET	GCM	Wolf	Expt.[a]
	4	2	0.0003		0.0#	
	4	4	0.3×10^{-5}*		0.0#	
	4	6	0.002			
	6	4	0.0004*			
	6	6	0.3×10^{-5}			
	6	8	0.003*			
$0_2^+ \to \gamma$	0	2	0.472*	0.337		
	2	2	0.001*		0.036#	
	2	3	0.235*			
	2	4	0.087*			
	4	2	0.1×10^{-6}		0.0#	
	4	3	0.0001*		0.014#	
	4	4	0.0005		0.014#	
	4	5	0.173*			
	6	7	0.147			
others	0_3	2_1	0.061	0.082	0.0#	
	0_3	2_2	0.001*		0.047#	
	0_3	2_3	0.001		0.0#	
	0_4	2_1	0.7×10^{-8}		0.7×10^{-4}#	
	0_4	2_2	0.0009		0.0#	
	0_4	2_3	0.009		0.0054#	
	0_4	2_4	0.550	0.489		
	2_4	2_3	0.404*	0.381		
	2_4	2_4	0.041	−0.205		
	2_4	4_3	0.133*			
	2_5	0_3	0.202*			
	2_5	2_5	−0.226			
	3_2	2_4	0.309*			
	3_2	4_4	0.171			
	4_3	2_1	0.8×10^{-7}		0.0#	
	4_3	2_2	0.0001		0.032#	
	4_3	2_3	0.0004		0.0036#	
	4_3	3_1	0.280*		0.21	
	4_3	4_1	0.5×10^{-4}		0.0036#	
	4_3	4_2	0.238*	0.222	0.18	
	4_3	4_3	0.095	0.338		
	4_3	6_1	0.005		0.0036	
	4_5	2_4	0.194*			
	4_5	4_4	0.245			
	5_2	4_3	0.382			
	5_2	5_1	0.129			
	6_3	4_3	0.236			
	6_3	5_1	0.099*			
	6_3	6_2	0.217			
	6_3	6_3	0.034			
	6_5	5_2	0.404*			
	6_5	6_3	0.155			
	6_5	6_5	0.123			
	7_2	5_2	0.229*			
	7_2	6_3	0.184*			
	8_3	6_3	0.352			
	8_3	7_1	0.048*			
	8_3	8_2	0.189*			
	8_3	8_3	0.055			

[a]Experimental data, except for $4_\gamma \to 4_g$ transition, are taken from Ref. [16].
[b]Reference [49].

TABLE II. $B(E2)$ ratios in ^{128}Ba.

I_i	I_f	BET	Expt.
0_2	$2_2/2_1$	88.1	<560[a]
0_3	$2_2/2_1$	0.021	<0.7[a]
			<1[b]
0_3	$2_3/2_1$	0.017	<33[b]
2_2	$0_1/2_1$	0.8×10^{-4}	0.12(1)[b]
			0.11(3)[c]
2_3	$0_1/0_2$	0.0012	0.0025(5)[b]
2_3	$2_2/0_2$	0.52	<0.18[b]
2_3	$4_1/0_2$	0.014	0.03(1)[b]
3_1	$2_1/2_2$	0.0004	0.06(1)[b]
3_1	$4_1/2_2$	0.38	0.16(3)[b]
4_2	$2_1/2_2$	0.0002	0.019(3)[b]
			0.015(3)[c]
4_2	$3_1/2_2$	0.012	
4_2	$4_1/2_2$	0.88	0.28(5)[b]
			0.26(5)[c]
4_3	$2_2/2_3$	0.41	0.5(3)[b]
4_3	$4_2/3_1$	0.85	1.1(2)[b]
4_4	$2_2/4_1$	0.044	<0.08[b]
5_1	$4_2/3_1$	0.45	
5_1	$4_1/4_2$	0.0014	
6_1	$4_2/4_1$	0.0010	
6_2	$4_1/4_2$	0.0001	0.008(2)[c]
6_2	$5_1/4_2$	0.0082	
8_1	$6_2/6_1$	0.0010	
8_2	$6_1/6_2$	0.0002	0.008(6)[c]

[a]Reference [14].
[b]Reference [15].
[c]Reference [49].

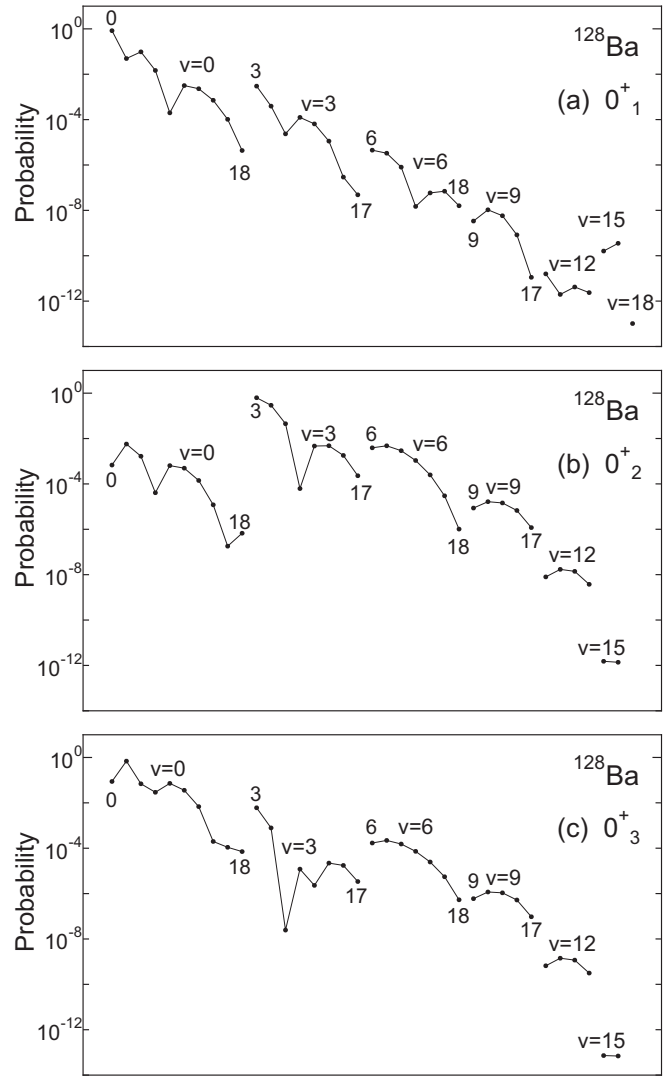

FIG. 4. Probability distributions of the boson numbers N and the seniorities v in the theoretical wave functions for 0^+_1, 0^+_2, and 0^+_3 states in ^{128}Ba. Components of the same seniority are separately accumulated and connected in the ascending order of N. The numbers attached at some beginning or ending points represent the boson numbers.

feature may be partly explained by the O(6) limiting case of IBM or alternatively by rotationally induced changes in the single-particle level structure at spins higher than $I^\pi = 4^+$. However, still today, it remains an important challenge for nuclear structure theories to explain it microscopically [45,46] and warrants further theoretical and experimental studies.

For comparison, the results of the IBM studied by Wolf *et al.* [15] are also listed in Table I. The present BET results show rather small $B(E2)$ values for most of the transitions which are forbidden in the pure O(6), and results of the two boson theories resemble each other at least for those allowed $B(E2)$ values where predictions of Ref. [15] are available. It should be noted here, however, that the two boson theories not always predict similar results since the origin of the boson description of the present BET, which starts from the microscopic fermion Hamiltonian, is rather different from that of the IBM.

In Table II, theoretical $B(E2)$ ratios obtained in the present BET calculation of ^{128}Ba are listed and are compared with experimental data. While most of the values presented are qualitatively reproduced by the model, the calculated $B(E2)$ ratio of the 2_2 decay to $0_1/2_1$ states differs with more than three orders of magnitude to the experimental value. The outstanding smallness of the theoretical ratio can be attributed to the forbidden nature of the theoretical $B(E2 : 2^+_2 \rightarrow 0^+_1)$ transition (Table I). In fact, this transition is forbidden in both purely vibrational and purely γ-unstable models as well as the O(6) limit, and the present theoretical situation seems to posses the nature too strongly. Since for such a numerical ratio deduced from prominently small $B(E2)$ value(s), the fluctuation of a calculated $B(E2)$ ratio due to possible ambiguities of parameters in the original fermion Hamiltonian tends to become relatively large, this difficulty may be partly remedied by a possible adjustment of the parameters.

Figure 4 illustrates the probability distributions of the boson numbers N and the seniorities v in the theoretical wave functions for 0^+_1, 0^+_2, and 0^+_3 states, and Fig. 5 presents the same illustration but for 2^+_1, 2^+_2, and 2^+_3 states. First of all, from these figures one can verify the selection rules [47] for the possible values of v are satisfied. One can also clearly see in these figures to what degree the boson wave functions converge in terms of v and N in the present numerical calculations.

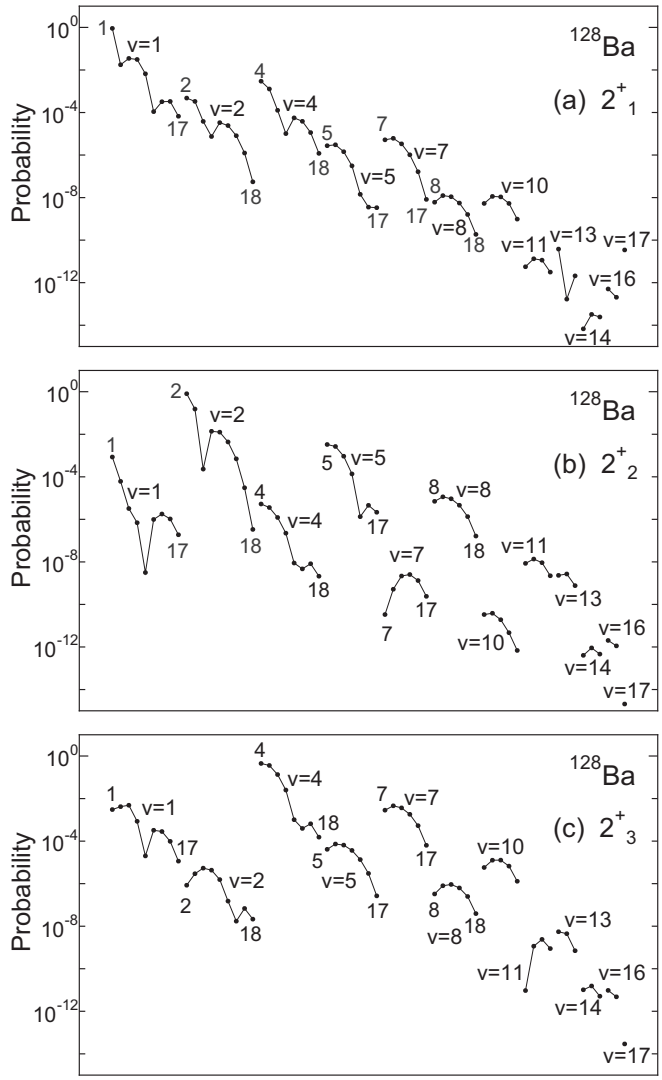

FIG. 5. The same as in Fig. 4 but for 2^+_1, 2^+_2, and 2^+_3 states in ^{128}Ba.

In Fig. 4, the structure of the BET wave functions of the lowest three 0^+ states are compared with each other. As for the seniority component, it is seen that, for the ground state, and also for the 0^+_3 state, the main contribution comes from $v = 0$ followed by $v = 3,6,9,\ldots$, while for the 0^+_2 state that comes from $v = 3$ followed by $v = 0,6,9$ and so on. Within the $v = 0$ component of the ground state, with respect to the boson number, the main contribution comes from $N = 0$ followed by $N = 4,2,6,\ldots$, thus the leading component of the ground state is $|N,v) = |0,0)$ followed by $|4,0)$, $|2,0)$, $|6,0)$ and so forth.

From Fig. 5 one sees that, in terms of the seniority component, major contributions to the BET wave functions come from $v = 1,4,2,7,\ldots$, $v = 2,5,1,8,\ldots$, and $v = 4,1,7,5,\ldots$ for 2^+_1, 2^+_2, and 2^+_3 states, respectively. Within the $v = 1$ component of the 2^+_1 state, with respect to the boson number, the main contribution comes from $N = 1$ followed by $N = 5,7,3,\ldots$, thus the leading component of the 2^+_1 state is $|N,v) = |1,1)$ followed by $|5,1)$, $|7,1)$, $|3,1)$ and so forth.

TABLE III. Major components in distributions of the quantum numbers v and N, characterizing theoretical wave functions, are listed in descending order for 0^+_1, 0^+_2, 0^+_3, 2^+_1, 2^+_2, and 2^+_3 states in ^{128}Ba. Results of the present work (BET) are compared with the predictions of GCM [4].

		BET	GCM
0^+_1	v	0,3,6,9, . . .	0,3,6,9, . . .
0^+_1	N	0,4,2,6, . . .	2,0,4,5, . . .
0^+_2	v	3,0,6,9, . . .	3,0,6,9, . . .
0^+_2	N	3,5,7,2, . . .	3,6,2,4, . . .
0^+_3	v	0,3,6,9, . . .	
0^+_3	N	2,0,4,8, . . .	
2^+_1	v	1,4,2,7, . . .	1,4,2,7, . . .
2^+_1	N	1,5,7,3, . . .	3,1,4,5, . . .
2^+_2	v	2,5,1,8, . . .	2,5,1,8, . . .
2^+_2	N	2,4,8,10, . . .	2,4,5,3, . . .
2^+_3	v	4,1,7,5, . . .	
2^+_3	N	4,6,8,10, . . .	

In Table III, structures of collective wave functions are summarized for 0^+_1, 0^+_2, 0^+_3, 2^+_1, 2^+_2, and 2^+_3 states in terms of the distributions of the quantum numbers v and N, and are compared with the predictions of the GCM calculated by Petkov *et al.* (Fig. 7 in Ref. [4]). As for the states where the GCM wave functions are available, i.e., for 0^+_1, 0^+_2, 2^+_1, and 2^+_2 states in ^{128}Ba, the major components in distributions of the seniorities v in the BET wave functions are in good agreement with those in the GCM wave functions. One can find differences, however, in the structure of the 0^+_1 and 2^+_1 states of the ground band: in the BET wave functions, as already mentioned, the leading component of the 0^+_1 state is $|N,v) = |0,0)$ and that of the 2^+_1 state is $|N,v) = |1,1)$, while in the GCM wave function, the frequency distributions of their quantum numbers ν and λ, which correspond to our N and v, show maxima at $\nu = 2$ and $\lambda = 0$ for the 0^+_1 state and at $\nu = 3$ and $\lambda = 1$ for the 2^+_1 state.

Remarkable similarities between the two theories can be found in the descriptions for the states in the quasi-γ band: for the wave function of the 2^+_2 state, in the distribution of the seniority quantum number, four major contributions in descending order are $v = 2$, 5, 1, 8, and in terms of the phonon number the most important two components are $N = 2$, 4 in both the GCM and the BET calculations, and as one can see in Table I intraband $B(E2 : I \rightarrow I - 2)$ transitions in the quasi-γ band have rather close values in both the theories and compare well with experiment.

Concerning the nature of the low-lying 0^+ states, in the present results, the main contribution to the 0^+_2 state of ^{128}Ba comes from the three-phonon component, and the two-phonon component is rather dominant in the 0^+_3 state. This result for the 0^+_2 state is compatible with the GCM calculations of Ref. [4] where, although the structure of the 0^+_3 state was not listed, the most dominant component in the 0^+_2 state of ^{128}Ba was reported to be the state with a phonon triplet coupled to zero angular momentum.

For the levels of the 0_2^+ band, one sees in Tables I and II that calculated $B(E2)$ transition strengths to the g.s.b. are rather small compared to those to the quasi-γ band, which implies that it is difficult to interpret the 0_2^+ state as a β bandhead. This property of the calculated $B(E2)$ can be understood as follows: In terms of the α-boson representation, the main component of the wave function of 0_2^+ state of ^{128}Ba is expressed as $|0_2^+) \sim (\alpha^\dagger\alpha^\dagger\alpha^\dagger)|0)$, while that of the 2_2^+ state is $|2_2^+) \sim [\alpha^\dagger\alpha^\dagger]^{(2)}|0)$, where $(\alpha^\dagger\alpha^\dagger\alpha^\dagger) = (\alpha^\dagger \cdot [\alpha^\dagger\alpha^\dagger]^{(2)})$ and $|0)$ is the α-boson vacuum. Since the leading-order term of the $E2$ transition operator in the BET is $T(E2) \sim (\alpha^\dagger + \alpha)$, the transition from the 0_2^+ state to the 2_2^+ state becomes strong.

In the wave function of the 0_2^+ state, we find a considerable amount of such a component of a collective α-boson excitation built on the 2_2^+ state. In Ref. [48], Casten and von Brentano proposed the interpretation that the lowest $K = 0$ intrinsic excitation of deformed nuclei is not a β vibration but rather a collective phonon built on the γ vibration. Although ^{128}Ba is a transitional nucleus and for deformed nuclei it must be fair to investigate the precision of the proposal elsewhere separately, in the present numerical results there seems to be a possibility that the 0_2^+ state of ^{128}Ba possesses similarity to the state discussed in Ref. [48]. In addition, the present BET analyses seem to suggest for ^{128}Ba a certain amount of the β vibrational component may exist in the 0_3^+ state. In fact, as already discussed, the major component of the wave function of the 0_3^+ state is $|2,0)$ and as one sees in Tables I and II the 0_3^+ state shows an $E2$ transition to the ground band, although the calculated energy of the 0_3^+ state seems rather high.

However, at present, it is premature to interpret that dominant component of the 0_2^+ state of ^{128}Ba is the double-γ phonon, because the branching ratio $R \equiv B(E2 : 0_2^+ \to 2_2^+)/B(E2 : 0_2^+ \to 2_1^+)$ has not been precisely determined yet [49], although one can estimate its upper limit from the experimental data of Ref. [14] as $R < 560$, and the theoretical value in this work is $R = 88.1$. Moreover, since the α-boson wave functions dress microscopic effects of mode-mode couplings, where contributions of pairing-vibrational modes as well as those of some noncollective quasiparticle excitations are included partially, and it is often the case that pairing-vibrational character is important to understand the nature of the low-lying 0^+ states, the above discussion for the major components of relevant wave functions in terms of only the α-boson representation is primitive, and further analyses to extract precise mixing ratios of different modes of motions are necessary.

The low-lying 0^+ states probably posses rather complex characteristics. To understand their nature microscopically, extensive investigations, including analyses of two-nucleon transfer strengths [50], which provide more precise identification of components of the wave functions in terms of the β vibration, the pairing-vibration, and the (two-phonon) γ vibration, among others, are called for. Results of our further analyses will be reported in a separate presentation.

IV. SUMMARY AND CONCLUSIONS

The low-lying quadrupole collective states of ^{128}Ba are studied by means of the BET with self-consistent effective interactions. The calculated potential surface has two minima, one on the prolate side and the other on the oblate side with rather small difference in depth compared to the energy of the zero-point oscillation, which implies strong softness or instability for the γ deformation.

The energies of the ground-state band and staggering of the quasi-γ band are qualitatively reproduced, although the energy of the band head 2^+ state of the quasi-γ band is too low, and the inversion of the orders of even- and odd-spin states above the 7_γ^+ state is not reproduced. Concerning the descriptions of the electromagnetic properties, the intraband $B(E2 : I \to I-2)$ transitions in the quasi-γ band are well described, but for the ground-state band the features of relatively high $B(E2 : 4_1^+ \to 2_1^+)$ value and the following drop are not reproduced.

The descriptions of the structures of the collective wave functions are investigated and compared to the results of the GCM. For 0_1^+, 0_2^+, 2_1^+, and 2_2^+ states in ^{128}Ba, the major components in distributions of the seniorities v in the present BET wave functions are in good agreement with those in the GCM wave functions. Remarkable similarities between the two theories can be found in the descriptions for the states in the quasi-γ band, while differences exist in the structure of the 0_1^+ and 2_1^+ states of the ground band. The present results indicate that the main contribution to the 0_2^+ state of ^{128}Ba comes from the three-phonon component, which is compatible with the prediction of the GCM, while the two-phonon component is rather dominant in the 0_3^+ state.

In summary, the present investigation gives several useful pieces of information about the structure of wave functions of the low-lying collective states in ^{128}Ba and provides an important step towards the microscopic description of nuclei in this mass region.

[1] T. Kishimoto and T. Tamura, Nucl. Phys. A **270**, 317 (1976).
[2] S. G. Rohoziński, J. Dobaczewski, B. Nerlo-Pomorska, K. Pomorski, and J. Srebrny, Nucl. Phys. A **292**, 66 (1977).
[3] R. F. Casten and P. von Brentano, Phys. Lett. B **152**, 22 (1985).
[4] P. Petkov, A. Dewald, and W. Andrejtscheff, Phys. Rev. C **51**, 2511 (1995).
[5] N. Hinohara, Z. P. Li, T. Nakatsukasa, T. Nikšić, and D. Vretenar, Phys. Rev. C **85**, 024323 (2012).
[6] D. A. Arseniev, A. Sobiczewski, and V. G. Soloviev, Nucl. Phys. A **126**, 15 (1969).
[7] K. Pomorski, B. Nerlo-Pomorska, I. Ragnarsson, R. K. Sheline, and A. Sobiczewski, Nucl. Phys. A **205**, 433 (1973).
[8] I. Ragnarsson, A. Sobiczewski, R. K. Sheline, S. E. Larsson, and B. Nerlo-Pomorska, Nucl. Phys. A **233**, 329 (1974).
[9] D. R. Zolnowski and T. T. Sugihara, Phys. Rev. C **16**, 408 (1977).
[10] N. V. Zamfir and R. F. Casten, Phys. Lett. B **260**, 265 (1991).
[11] P. F. Mantica, Jr., B. E. Zimmerman, W. B. Walters, J. Rikovska, and N. J. Stone, Phys. Rev. C **45**, 1586 (1992).
[12] J. Yan, O. Vogel, P. von Brentano, and A. Gelberg, Phys. Rev. C **48**, 1046 (1993).

[13] W. Lieberz, A. Dewald, W. Frank, A. Gelberg, W. Krips, D. Lieberz, R. Wirowski, and P. Von Brentano, Phys. Lett. B **240**, 38 (1990).
[14] M. Asai, T. Sekine, A. Osa, M. Koizumi, Y. Kojima, M. Shibata, H. Yamamoto, and K. Kawade, Phys. Rev. C **56**, 3045 (1997).
[15] A. Wolf, N. V. Zamfir, M. A. Caprio, Z. Berant, D. S. Brenner, N. Pietralla, R. L. Gill, R. F. Casten, C. W. Beausang, R. Kruecken, K. E. Zyromski, C. J. Barton, J. R. Cooper, A. A. Hecht, H. Newmann, J. R. Novak, and J. Cederkall, Phys. Rev. C **66**, 024323 (2002).
[16] P. Petkov, A. Dewald, R. Kühn, R. Peusquens, D. Tonev, S. Kasemann, K. Zell, P. von Brentano, D. Bazzacco, C. Rossi-Alvarez, G. de Angelis, S. Lunardi, P. Pavan, and D. R. Napoli, Phys. Rev. C **62**, 014314 (2000).
[17] T. Komatsubara, T. Hosoda, H. Sakamoto, T. Aoki, and K. Furuno, Nucl. Phys. A **496**, 605 (1989).
[18] K. Uchiyama, H. Sakamoto, and K. Furuno, RIKEN Accelerator Progress Report **33**, 73 (2000).
[19] H. Sakamoto, Phys. Rev. C **64**, 024303 (2001).
[20] T. Kishimoto and T. Tamura, Nucl. Phys. A **192**, 246 (1972).
[21] T. Kishimoto and T. Tamura, Phys. Rev. C **27**, 341 (1983).
[22] H. Sakamoto, Phys. Rev. C **52**, 177 (1995).
[23] H. Sakamoto and T. Kishimoto, Nucl. Phys. A **486**, 1 (1988).
[24] H. Sakamoto and T. Kishimoto, Nucl. Phys. A **528**, 73 (1991).
[25] S. G. Nilsson, C. F. Tsang, A. Sobiczewski, Z. Szymański, S. Wycech, C. Gustafson, I.-L. Lamm, P. Möller, and B. Nilsson, Nucl. Phys. A **131**, 1 (1969).
[26] B. R. Mottelson, *Nikko Summer School Lectures*, NORDITA Pub. 288 (1967).
[27] A. Bohr and B. R. Mottelson, *Nuclear Structure* (Benjamin, New York, 1975), Vol. II, Chap. 6.
[28] T. Kishimoto, J. M. Moss, D. H. Youngblood, J. D. Bronson, C. M. Rozsa, D. R. Brown, and A. D. Bacher, Phys. Rev. Lett. **35**, 552 (1975).
[29] T. Kishimoto, in *Proceedings of the International Conference on Highly Excited States in Nuclear Reactions* (RCNP, Osaka, 1980), p. 377.
[30] T. Kishimoto, T. Tamura, and T. Kammuri, Prog. Theor. Phys. Suppl. **74-75**, 170 (1983).
[31] H. Sakamoto and T. Kishimoto, Nucl. Phys. A **501**, 205 (1989); **501**, 242 (1989).
[32] E. R. Marshalek, Phys. Rev. Lett. **51**, 1534 (1983); Phys. Rev. C **29**, 640 (1984); Phys. Lett. B **244**, 1 (1990).
[33] M. Matsuo and K. Matsuyanagi, Prog. Theor. Phys. **78**, 591 (1987).
[34] S. A. Stotts and T. Tamura, Phys. Rev. C **40**, 2342 (1989).
[35] H. Aiba, Prog. Theor. Phys. **84**, 908 (1990).
[36] K. Yamada, Prog. Theor. Phys. **89**, 995 (1993).
[37] J. Copnell, K. Kumar, S. J. Robinson, and C. Tenreito, J. Phys. G **18**, 1943 (1992).
[38] H. Sakamoto and T. Kishimoto, Phys. Lett. B **245**, 321 (1990).
[39] T. Tamura, K. J. Weeks, and V. G. Pedrocchi, Phys. Rev. C **23**, 1297 (1981).
[40] S. Okubo, Prog. Theor. Phys. **12**, 603 (1954).
[41] N. Fukuda, K. Sawada, and M. Taketani, Prog. Theor. Phys. **12**, 156 (1954).
[42] A. Messiah, *Quantum Mechanics* (North-Holland, Amsterdam, 1961), Vol. II, Chap. XVI.
[43] K. Suzuki and R. Okamoto, Prog. Theor. Phys. **71**, 1221 (1984).
[44] H. Feshbach, Ann. Phys. (NY) **5**, 357 (1958); **19**, 287 (1962).
[45] A. Bohr and B. R. Mottelson, Phys. Scr. **22**, 468 (1980).
[46] A. Faessler, Nucl. Phys. A **396**, 291 (1983).
[47] E. Chacón, M. Moshinsky, and R. T. Sharp, J. Math. Phys. **17**, 668 (1976).
[48] R. F. Casten and P. von Brentano, Phys. Rev. C **50**, R1280 (1994).
[49] Z. Elekes and J. Timar, Nucl. Data Sheets **129**, 191 (2015).
[50] S. Pascu, G. Cáta-Danil, D. Bucurescu, N. Márginean, N. V. Zamfir, G. Graw, A. Gollwitzer, D. Hofer, and B. D. Valnion, Phys. Rev. C **79**, 064323 (2009).